The copper carbonyl complexes revisited: Why are the infrared spectra and structures of copper mono and dicarbonyl so different?

Mohammad Esmaïl Alikhani, Laurent Manceron

The copper carbonyl complexes revisited: why are the infrared spectra and structures of copper mono and dicarbonyl so different?

Mohammad Esmail Alikhani[a] and Laurent Manceron[b*]

a- Sorbonne Universités, UPMC Univ. Paris 06, MONARIS, UMR 8233, Université Pierre et Marie Curie,4 Place Jussieu, case courrier 49, F-75252 Paris Cedex 05, France

and

b- CNRS, MONARIS, UMR 8233, Université Pierre et Marie Curie, 4 Place Jussieu, case courrier 49, F-75252 Paris Cedex 05 and Synchrotron Soleil Ligne AILES, BP 48, 91192 Cedex Gif-sur-Yvette, France

**Corresponding author (laurent.manceron@synchrotron-soleil.fr)*

Abstract

New Infrared absorption data have been obtained using isolation in solid argon and neon on copper carbonyl molecules, CuCO and $Cu(CO)_2$, two very reactive molecules. For CuCO, all three fundamentals are now observed and it presents an unusually large matrix effect, in line with former results indicating a weak metal carbon interaction and a large total dipole moment. With help of isotopic effects, new data indicates unambiguously that $Cu(CO)_2$ is linear and presents a notably stronger metal-carbon interaction than CuCO. Quantum chemical calculation have been carried out at the CCSD(T) level for determining energies and structural properties, as well as spectroscopic observables. The results enable an assessment of the high stability of the $Cu(CO)_2$ molecule (first bond dissociation energy of 66 kJ/mole) which suggest that observation at room temperature is possible and give a first evidence of Renner effect on a penta-atomic molecule.

Keywords : CuCO, $Cu(CO)_2$, far infrared, infrared spectrum, structure, bonding analysis, Renner-Teller effect.

Introduction

One chief application of rare gas matrix isolation (MI) is the trapping of reactive or unstable species, as large amounts (μmole range) of radicals or transient species can be stabilized in solid solution within a thin solid rare gas slab, enough to permit the use of a combination of various spectroscopic techniques [1]. Among the pioneers in the field [2] who developed co deposition of metal atoms with small molecules to model various reactions, M. Jacox was among the first to use alkali atoms to generate molecular anions by charge transfer mechanisms [3,4]. Among many contributions, she was one of the first to implement a variety of spectroscopic techniques, including far infrared spectroscopy, taking advantage of the fact that these reactive species are trapped and made long-lived. In more recent years, with the generalization of *ab initio* and DFT quantum chemical (QC) calculations and the improvement of its predictive power for spectroscopic properties, M. Jacox warned against the danger of relying solely on apparent matches between QC-predicted vibrational frequencies for making definite species identifications or transitions assignments and advocated combining and cross-checking these with extensive isotopic effects [5]. These principles have been an inspiration to many and in particular to us here.

Neutral copper carbonyl complexes have been the object of many studies and came across to be intriguing objects, laboratory models for a number of concepts. For the copper mono-carbonyl after several conflicting studies, a consensus has emerged that it is a weakly bound, quite floppy species and a non-conventional, bent structure [6-9]. The situation for the di-carbonyl species is quite different: experimental data are much scarcer and all theoretical studies converge in predicting a much more strongly bound species with a linear structure. It has been observed in three separate infrared absorption MI studies, following the brief initial report of Ogden [10], the more complete work on binary copper carbonyl complexes by Huber and coworkers [11] who detected a very intense CO stretching fundamental vibration and, more recently, in the work by Andrews and coworkers [12] on the isolation of neutral and ionic copper carbonyls and the frequencies for this mode re-measured in solid argon and neon. On the basis of isotopic effects and of the inactivity of the second, symmetrical CO stretching, it was concluded that this species should be centro-symmetrical, presumably linear. Remarkably, it was not observed in two separate ESR MI studies by Kasai and Jones [13] and Chenier and coworkers [14], in samples where the other binary carbonyls (CuCO and $Cu(CO)_3$) were observed. This negative result was interpreted as a proof that this molecule is, indeed, linear and having a $^2\Pi$ ground state, in which case it is expected to be ESR-silent. In 1995, V. Barone, using various DFT-based calculations, predicted the electronic structures, energies, geometries and some spectroscopic vibrational properties of the CuCO, $Cu(CO)_2$ and $Cu(CO)_3$ series [15], predicting remarkably well the bent structure of CuCO and that $Cu(CO)_2$ should revert to linearity with a $^2\Pi$ ground state. Even more recently, Cerón and Mendizabal examined in detail for the first time using high level ab initio methods, ranging from MP2 to CCSD(T), the reasons for the change in bonding strength when going from CuCO to $Cu(CO)_2$ [16]. In particular, they showed that the low stability of the copper-monocarbonyl [17] could be perfectly explained by calculating the induction and dispersion contributions, at the highest level of theory. In a parallel publication, Wu et al. reached quite similar conclusions [18] and compared the performances of several DFT methods. None of these theoretical studies confronted their predictions, however, to the available

experimental data on the low frequency metal-ligand stretching and bending modes [19], most sensitive to the nature of the bonding and the chosen QC method.

In the course of studies devoted to the observation of the low frequency stretching and bending modes of transition metal carbonyls, new data pertaining to $Cu(CO)_2$ and $Cu(CO)_3$ were observed in our laboratory. If the data concerning the $Cu(CO)_3$ complex match reasonably well the former DFT predictions [15] and are readily understandable in terms of a vibrational spectrum of a trigonal, D_{3h} symmetry species, the data concerning $Cu(CO)_2$ present specific features which cannot be readily understood in terms of a purely vibrational spectrum of a linear species. In fact, with a $^2\Pi$ ground state, $Cu(CO)_2$ constitutes a rare example of five-atomic molecule with a Renner-Teller effect. The goal of this contribution is thus three-fold: make use of the unique possibilities of MI to investigate the IR spectroscopy of a linear five-atomic molecule with a Renner-Teller effect, give spectroscopic indicators of the bonding strength in $Cu(CO)_2$ and describe the specific features of the bonding with topologic arguments at the required level of theory.

Experimental details.

Samples containing copper carbonyl complexes were formed by co-condensing Cu vapor and dilute CO-Ar or Ne mixtures (0.5-16% CO/Ar or 200-2000ppm O_2/Ne), onto one of six flat, highly polished, Rh-plated copper mirrors maintained between 3 and 15K using a pulse-tube, closed-cycle cryogenerator (Cryomech PT405, Syracuse, USA), the experimental procedures are described in Reference 20.

Copper wire (99.998% purity, Alpha Aesar) was wrapped around a tungsten filament, and heated at 800-900°C to generate the Cu metal vapour. The metal deposition rate was carefully monitored with the aid of a quartz microbalance and was varied from 1 to 10 nanomol/min. High purity Neon or Argon (Air Liquide, France; 99,995%), carbon monoxide (Air Liquide, France; 99,998%), ^{13}CO (CEA, Saclay, France; 99 % ^{13}CO including 9 % $^{13}C^{18}O$), $^{12}C^{18}O$ (MSD; 98 % ^{18}O) were used to prepare the gas mixtures. Survey absorption spectra were recorded between 10000 and 50 cm^{-1} *on the same samples* using a Bruker 120 FT spectrometer with 0.1 cm^{-1} resolution and different beam splitter/sources/detector/window combinations covering the far infrared to near infrared range, as detailed in Ref. 20. For selected spectral ranges, high resolution scans were acquired with 0.02 cm^{-1} resolution. Diffusion experiments were performed by annealing the samples to 9 - 10K (neon) or 25-30 K (argon) *in the dark*, the sample facing an 80K radiation shield.

Computational details:

Geometrical optimizations, vibrational frequency and Natural Bonding Orbital (NBO) calculations have been performed using the Gaussian 09 quantum chemical package [21]. Optimized molecular structures and harmonic vibrational frequency of CO, CuCO, and $Cu(CO)_2$ compounds were determined by means of the coupled-cluster single and doubles and with perturbative triples [CCSD(T)] method with the 6-311+G(2d) Pople's basis set, as implemented in Gaussian 09 package. Additional optimization and harmonic vibrational frequency computations were carried out with the popular B3LYP functional.

The NBO figures have been obtained using the Multiwfn Version 3.3.5 software[22].The nature of chemical bonding has been investigated in the framework of the AIM ("Atoms In Molecul" of Bader [23]) topological approach with help of the AIMAll code [24].

We recall that the "wfx" files, necessary to the AIM calculations, were obtained with a CCSD/6-311+G(2d) single-point calculation at the CCSD(T)/6-311+G(2d) optimized geometry and using the "Density=Current".

Experimental Results

Figure 1 presents the infrared spectra observed for CuCO isolated in solid argon and neon. As noted earlier, the ν_2 and ν_3 metal-ligand bending and stretching fundamentals of this species are at low frequency [19]. Also, notably, while the ν_1 mode experiences a small blue shift from 2010 to 2034 cm-1 (1.2%) from argon to neon, the low frequency modes experience a very large redshift (322.7 to 294.9 cm-1, thus -9.7%, and 207.5 to 176.7 cm-1, thus -17%). These latter values indicate an anomalously large matrix effect. For most rigid molecules, the compilation of matrix results by M. Jacox indicates an average gas-to matrix shift of –2% for argon and less than 0.4% for neon [1]. A large matrix effect for argon is expected when a highly polar molecule is embedded in this polarizable medium, especially for weakly bonded species [25]. In solid neon, much less polarizable, more reliable data are obtained and the frequencies observed here can serve as better reference point for QC calculations.

Remarkably, the known $Cu(CO)_2$ absorptions present only a slight argon to neon blue shift (0.8 to 0.1%, +0.4% on average), characteristic for a rigid, more covalently bound molecule, thus confirming that the bonding evolves markedly by adding a second carbonyl group (see theoretical section below).

As noted by earlier workers, the $Cu(CO)_2$ and $Cu(CO)_3$ species are favored in samples with relatively high CO content (typically 2 to 4 % in argon) and can be easily discriminated in the CO stretching vibration region, between 2100 and 1850 cm-1, from CuCO absorption with stepwise CO concentration increase (figure 1 of reference 19), with $Cu(CO)_2$ growing after CuCO, and $Cu(CO)_3$ appearing next. It is thus straightforward to discriminate and group infrared absorptions pertaining to $Cu(CO)_2$ and $Cu(CO)_3$ from their growth behavior. All absorptions observed in argon present a multiple trapping site pattern, common for the medium [1,2]. For the sake of simplicity, we will only quote further the main trapping site frequencies. In neon, the absorptions are quite sharp and present a single trapping site after deposition. In this study, we observed nine new bands for various isotopic precursors of $Cu(CO)_2$ (table 1) and ten new bands for $Cu(CO)_3$ (table 2). The new data observed emerged mainly in two spectral regions: the mid-to near infrared above 2500 cm^{-1} and the mid- to far infrared between 800 and 100 cm^{-1}. For each band observed with a single isotopic precursor characteristic patterns emerge with ^{12}CO + ^{13}CO isotopic mixtures : triplets for $Cu(CO)_2$ and quartet for $Cu(CO)_3$ (Figures 2-7), as expected for species with two, respectively three, carbonyl groups.

The data for $Cu(CO)_3$ (table 2) are only mentioned here and will not be discussed further as this molecule is not the objective of this work.

For $Cu(CO)_2$, the near infrared features must involve overtones or combinations involving the high frequency carbonyl stretching modes. From simple symmetry consideration only $\nu_1+\nu_3$, $\nu_2+\nu_3$, $\nu_1+\nu_4$ can produce IR active transitions for the stretching motions, while combination of $\nu_3+\nu_5$, $\nu_1+\nu_6$ (with ν_5 and ν_6 being the trans- and cis- Cu-C=O bending modes , respectively (figures 2 and 3). The frequencies for the various isotopic species for the strong ν_3 antisymmetrical CO stretching mode are known, and our experiments show here a weaker band at 2031.0 cm^{-1}, belonging to the dicarbonyl molecule, which also indicate that of the ν_1 symmetrical stretching for the Cu(CO)(^{13}CO) species (figure 4) for which the inversion center is no longer present and this motion slightly IR activated. This band is observed with an intensity ratio of about 0.034(9) with respect to the strongest, ν_3 antisymmetrical CO stretching mode at 1865.9 cm^{-1}. Thus, assignments of the bands at 3914.9, 2542.5 and 2297 cm^{-1} to the $\nu_1+\nu_3$, $\nu_2+\nu_3$ and $\nu_1+\nu_4$ transitions are fairly straightforward. This implies an X_{11} and X_{13} anharmonicity coefficients of 40.2 and 14.4 cm^{-1}, somewhat larger but in line with $Ni(CO)_2$, a comparable example [26]. Note that the relationship $X_{11} / X_{13} = 4$, true in the limit of the local mode model developed by Mills and Robiette [27], holds here only approximately, showing that ν_1 and ν_3 are not purely carbonyl stretching motions, but vibrations in which carbonyl and metal-carbon stretching motions are notably coupled. This also shows when examining the isotopic effects on ν_3, with a $^{12}C/^{13}C$ shift larger than the $^{16}O/^{18}O$ one, in spite of a smaller change in reduced mass, another sign of coupling [28]. Assignment of the weak band at 2542.5 cm^{-1} to the $\nu_1+\nu_4$ transition would place the ν_4, Σ_u symmetry band around 490 cm^{-1}.

In fact, in the low frequency region, a very weak band is observed near 493 cm-1 (figures 5 and 7), with a notably larger $^{16}O/^{18}O$ shift (-10.7 cm^{-1}) than $^{12}C/^{13}C$ (-3.5 cm^{-1}) , which can thus be assigned to the ν_4 mode. Further below, a much stronger band is observed near 247 cm^{-1}, with a large $^{12}C/^{13}C$ (-7.2 cm^{-1}) and a small $^{16}O/^{18}O$ (-1.9 cm^{-1}) isotopic effects, as expected for a Cu-C=O bending mode, which must involve the cis-C-C=O bending coordinate. Another band is, however, observed near 610 cm^{-1} with the same isotopic behaviour and, yet, about 15% of the intensity of the former, thus very unusually strong for a combination or overtone transition. Another very weak band is observed near 888 cm^{-1} with isotopic shifts comparable in *absolute* value (about -1.9 cm^{-1} $^{16}O/^{18}O$ shift and cm^{-1} -9,7 cm^{-1} $^{12}C/^{13}C$ shift), but very different in *relative* magnitude (-0.2% and -1%, respectively). This finds no simple explanation in a purely vibrational picture. To substantiate these considerations, Table 3 presents the results of a semi-empirical force field for calculations of the purely vibrational isotopic effects. Comparison is made with the frequencies observed for all four Σ_u and Σ_g stretching modes and the Π_u mode for the strong band at 247.4 cm^{-1}. The remaining Π_g modes are first fitted to the values proposed by Barone [15]. These results confirm that the proposed assignments for the stretching modes are fully consistent with the observed isotopic shifts. It is also possible to compute the intensity ratio, predictable with a zero order bond moment approximation, between the ν_1 symmetrical and the ν_3 antisymmetrical CO stretching modes. The value of 0.024 is consistent with experimental results. The model also indicate an important increase in the Copper-carbon bond force constant, from about 1 N/m in CuCO [19] to more than 2.5 N/m in $Cu(CO)_2$, a value characteristic for strong coordination bonds, close to that deduced for $Ni(CO)_2$ [26], but different from the smooth decrease from NiCO to $Ni(CO)_2$ and $Ni(CO)_4$ [30-32]. This is followed only by a moderate decrease in the CO bond force constant, from 16.6 to 15.2 N/m, and a qualitative change in geometry. These elements clearly indicate that a drastic change in the copper-carbonyl bonding nature takes place with the addition of a second carbonyl group. This motivates an examination of the bonding nature with the appropriate theoretical methods.

Theoretical Results

In their theoretical paper on the mono- and dicarbonyl, Ceron and Mendizabal showed that the stability of the copper-monocarbonyl could be perfectly explained by calculating the induction and dispersion contributions [16]. Consequently, the causes of the failure of the density functional -based methods, not taking into account correctly the dispersion energy, can be understood.

Accordingly, in order to investigate the $Cu(CO)_2$, the conclusions of reference 16 were followed and the CCSD(T) method retained. Theoretical geometrical, energetic and vibrational data are gathered in Table 1. For CuCO and $Cu(CO)_2$, the binding energy is calculated with respect to CO + Cu and CO + CuCO partners, respectively. The Cu-C bond length decreases by 0.14Å from mono- to dicarbonyl of copper. In parallel, we observe a very small increase in the C-O distance (0.004Å) from free CO to CuCO. However, addition of a second CO leads to a significant lengthening of the C-O bond length (0.011Å). Accordingly, we can easily conclude that the dispersion contribution is not the main cause of the $Cu(CO)_2$ stability.

Bonding analysis. In order to complete the NBO analysis of Mendizabal, we provide here the plot of the orbitals involving in the bonding between carbon monoxide and copper atom. They are displayed in Figure 8 and 9.

In the bent Cu-CO, the bonding interaction of carbon monoxide with copper consists of a concerted electron delocalization over orbitals of σ and π character. We note that the overlapping between σ(Cu) and two π*(CO) and σ*(CO) antibonding orbitals is different from zero, owing to the bent structure of Cu-CO. The two bonding driving forces are synergistic and stabilize the complex (D_0= -10.6 kJ/mol). However, as shown in Table 4, the net charge of Cu is very small (+0.017 e), but enough to polarize substantially the complex (with a dipole moment of 2.14 D calculated at CCSD/6-311+G(2d)//CCSD(T)/ 6-311+G(2d) level, using the Density=Current" keyword).

The AIM topological properties have been listed in Table 2. Changes in the Cu atomic charge and in the charge density at C-O and Cu-C bond critical points are in line with the NBO analysis. For instance, the charge density at the C-O bond critical point decreases by 0.005 and 0.019 e/$Å^3$ from free CO to CuCO, and to $Cu(CO)_2$. The most notable change occurs at the Cu-C bond critical point when we compare CuCO to $Cu(CO)_2$: it increases by 40%.

NBO and AIM analyses of $Cu(CO)_2$ evidenced the simultaneous existence of two phenomena: the formation of the Cu-C electron-shared bonds and the weakening of the CO bond. Thus, in the copper dicarbonyl molecule, copper forms a σ(Cu-C) covalent bond with each carbon monoxide leading to a high energetic stability (D_0= -66.9 kJ/mol). The CO bonds weaken upon formation of the dicarbonyl copper molecule, owing to the back-donation from lone pair π(Cu) to the antibonding π*(CO) orbital. These drastic changes in the bonding nature also improve considerably the abilities of DFT-based method for describing the bonding and predicting the spectroscopic properties.

*Vibrational frequencies and IR spectrum***.** As discussed above, $Cu(CO)_2$ could be, in contrast to CuCO, well described by the density functional bases method. In Table 5 are listed harmonic vibrational frequencies and some force constants calculated at the CCSD(T)/6-311+G(2d), and also some results calculated with B3LYP)/6-311+G(2d) method for CO and $Cu(CO)_2$ compound. The B3LYP results are reported in parentheses. The results presented here are in good agreement with experimental

findings for all four stretching modes and deserve no further special comment, except to note the exceptionnaly high predicted IR intensity for the ν_3 Σ_u-symmetry stretching mode, predicted near 2000cm-1 (vs. 1904 (neon) and 1891(argon) cm-1) (with near 4000 Km/mole), which explains its easy detection in early matrix work [10,11] and targets this mode for possible gas phase observation. The other Σ_u-symmetry stretching mode, ν_4, is predicted very weak, in line with the present experimental data (table 1).

A closer look at the situation indicates that, with a $^2\Pi_u$ ground state, the molecule should present a Renner-Teller situation [33], corresponding to case (A) as described in ref. [34] (figure 10) with the total energies of both electronic components of the degenerate state increasing as the molecular frame bends, resulting in changes in the bending vibrational frequencies for the vibronic states. In fact, in this case, QC calculations give in this case two different frequency values corresponding to the vibrations in the xz and yz planes (with z the molecular axis). This is caused by the fact that the potential surface for the $^2\Pi_u$ ground state splits upon bending into two components, with one corresponding to the plane for the unpaired electron of the electronic wave function. These frequencies are, however, different from the observables. A model for handling Renner-Teller effect in linear penta-atomic molecules has been developed by Peric and coworkers [35] in a thorough approach for the general case and applied to one vibronic transition of C_5^-. Our data are, of course, not sufficient to permit extraction of the seven parameters needed for attempting a reliable assignment, namely the frequencies ω_T (for the Cu-C=O trans-bending motion) , ω_{c1} (for the Cu-C=O cis-bending motion) , ω_{c2} (for the C-Cu-C=O bending motion) , ε_T, ε_{C1}, ε_{C2} and ε_{C12} the four Renner parameters (one for each of the bending and one connecting the two cis-bending motions, which can couple by symmetry). Noting that the second cis- C-Cu-C bending mode lies at much lower frequency than the other, Cu-C=O ones and that its Renner splitting seems small from QC calculations, we consider here only a first, very crude approximation: the C-Cu-C is considered rigid and the spin-orbit effect neglected. From the more reliable CCSD(T) calculations, ω_T = 343 cm^{-1} , ω_{c1} = 320 cm^{-1} , ε_T = -0.41 and ε_{C1} = 0.19 can be estimated using well-known approximations [36]. From this values and truncating the energy expressions developed in reference 35, we can compute energies of 310 cm^{-1} for the first transition to the(v_c=1, v_T=0) vibronic state and energies of 609 and 623 cm^{-1} to the (v_c=1, v_T=1)and (v_c=2, v_T=0) levels. Given the general overestimation of the frequencies in our QC calculations, we would thus suggest assignment of the observed transitions near 247 and 610 cm-1 to the transitions from ground to v_c = 1 and 2 states. In this simple picture, the very weak transitions observed near 888 cm-1 is not assigned and obviously requires a complete treatment of all vibronic effects.

Conclusions.

In this work new infrared absorption data have been observed for CuCO and $Cu(CO)_2$ molecules, produced by spontaneous reaction of copper atoms and carbon monoxide in solid argon and neon.

For CuCO, an important matrix effect and a very low copper-carbon stretching frequency both confirm the prediction that this species in a very weakly bound, polar complex. For $Cu(CO)_2$,the matrix effects are very small (less than 0.4% on average) indicating a strongly bound and non-polar

species, following the trends noted by M. Jacox [1,25]. Isotopic data on nine new bands, combined with semi-empirical and quantum chemistry calculations at the CCSD(T) level enable assignment of all stretching modes and a discussion of the transitions in the far infrared associated with bending motions. This study thus confirms former predictions that the molecule is linear and far-infrared data give evidence of a much stronger metal-carbon interaction. Also, a set of low-lying transitions cannot be explained in a purely vibrational picture, and is assigned to vibronic transitions caused by Renner-Teller effect, as predictable for a $^2\Pi_u$ ground state. To our knowledge, this is the first example of spectroscopic data on a neutral penta-atomic molecule with a Renner effect and illustrates the possibility of matrix-isolation to enable a first approach of these phenomena. Experimental and theoretical data converge in indicating a much stronger copper-carbon bond in the di-carbonyl than in the mono carbonyl and the bonding nature in both molecules is analyzed with topological methods. Finally, the relatively high stability (66 kJ/mole estimated here for the first bond dissociation energy) and the very high IR absorption intensity predicted for the ν_3 Σ_u-symmetry stretching mode, observed near 1904 cm-1 in solid neon, in a favourable IR domain might facilitate observation of the $Cu(CO)_2$ molecule in the gas phase, in a cold discharge experiment, for instance.

References

[1] M. Jacox, J. Phys. Chem. Ref. Data 32,1 (2003).

[2] Chemistry and Physics of Matrix-Isolated Species, edited by L. Andrews and M. Moskovits, Elsevier Science, Amsterdam, The Netherlands, 1989.

[3] L. Andrews, J. Phys. Chem. 73, 3922 ~1969. 54, 4935 ~1971!.

[4] M. E. Jacox and D. E. Milligan, Chem. Phys. Lett. 14, 518 ~1972.

[5] C. L. Lugez, W. E. Thompson, and M. E. Jacox, J. Chem. Phys. 115, 166 (2001).

[6] J.S.Tse, Ber. Bunsenges. Phys. Chem. 90, 906 (1986).

[7] L.A Barnes, M. Rosi ans C. Bauschlicher J. Chem. Phys,93, 609 (1990).

[8] R. Fournier , J. Chem. Phys, 98, 8041 (1993).

[9] P.Schwerdtfeger, G. Bowmaker, J. Chem. Phys, 100, 4487 (1993) and reference therein.

[10] J.S. Ogden, J. Chem. Soc. Chem. Comm. 978 (1971).

[11] H. Huber, E. Kündig, M. Moskovits, G.A.Ozin, J. Am. Chem. Soc. 97, 2097 (1975).

[12] M. Zhou and L. Andrews, J. Chem. Phys,111, 4548 (1999).

[13]P.H. Kasai, P.M. Jones, J. Am. Chem. Soc. 107, 813(1985).

[14] J.H. Chenier, C.A. Hampson, J.A. Howard, B. Mile J. Phys. Chem. 93, 114 (1989).

[15] V. Barone, J. Phys. Chem. 99, 11659 (1995).

[16] M. L. Cerón and F. Mendizabal, J. Chi. Chem. Soc., 48 (2003)

[17] M.A. Blitz, S.A. Mitchell, P.A. Hackett, J. Phys. Chem. 95 (1991) 8719.

[18] G. Wu, Y.W. Li, H.W. Xiang, Y.Y. XU, Y.H. Sun and H. Jao, J. Mol. Struct. Theochem. 637, 101 (2003).

[19] B. Tremblay, L. Manceron, Chem. Phys. 242, 235 (1999).

[20]- D. Danset, L. Manceron *J. Phys. Chem*. *A* , 107, 11324 (2003).

[21] Gaussian 09, Revision D.01, M. J. Frisch, G. W. Trucks, H. B. Schlegel, G. E. Scuseria, M. A. Robb, J. R. Cheeseman, G. Scalmani, V. Barone, B. Mennucci, G. A. Petersson, H. Nakatsuji, M. Caricato, X. Li, H. P. Hratchian, A. F. Izmaylov, J. Bloino, G. Zheng, J. L. Sonnenberg, M. Hada, M. Ehara, K. Toyota, R. Fukuda, J. Hasegawa, M. Ishida, T. Nakajima, Y. Honda, O. Kitao, H. Nakai, T. Vreven, J. A. Montgomery, Jr., J. E. Peralta, F. Ogliaro, M. Bearpark, J. J. Heyd, E. Brothers, K. N. Kudin, V. N. Staroverov, R. Kobayashi, J. Normand, K. Raghavachari, A. Rendell, J. C. Burant, S. S. Iyengar, J. Tomasi, M. Cossi, N. Rega, J. M. Millam, M. Klene, J. E. Knox, J. B. Cross, V. Bakken, C. Adamo, J. Jaramillo, R. Gomperts, R. E. Stratmann, O. Yazyev, A. J. Austin, R. Cammi, C. Pomelli, J. W. Ochterski, R. L. Martin, K. Morokuma, V. G. Zakrzewski, G. A. Voth, P. Salvador, J. J. Dannenberg, S. Dapprich, A. D. Daniels, Ö. Farkas, J. B. Foresman, J. V. Ortiz, J. Cioslowski, and D. J. Fox, Gaussian, Inc., Wallingford CT, 2009.

[22] Tian Lu, Feiwu Chen, Multiwfn: A Multifunctional Wavefunction Analyzer, J. Comp. Chem. 33, 580-592 (2012)

[23] Bader, R. F. W. Atoms in Molecules: A Quantum Theory; Clarendon: Oxford, U.K.; 1990.

[24] AIMAll (Version 14.06.21), Todd A. Keith, TK Gristmill Software, Overland Park KS, USA, 2014 (aim.tkgristmill.com).

[25] M. E. Jacox, J. Mol. Spectrosc. 113, 286 (1985).

[26] L. Manceron and M.E. Alikhani, Chem. Phys. 244 (1999) 215.

[27] I.M. Mills and A.G. Robiette, Mol. Phys. 56 (1985) 743.

[28] B. Tremblay and L. Manceron, Inorg. Chem., **47** (2008) 4531.

[29] H.A. Joly and L. Manceron, Chem. Phys., **226** (1998) 61.

[30] L.H. Jones, R.S. McDowell, M. Goldblatt, J. Chem. Phys. 48 (1968) 2663.

[31] P. Carsky, A. Dedieu, Chem. Phys. 103 (1986) 265.

[32] H.J. Himmel, L. Manceron. J. Chem. Soc. Dalton, Trans (2005) 2615.

[33] R. Renner, Z. Phys. 92 (1934) 172.

[34] T.J. Lee, D.J. Fox, H.F. Schaeffer III, R. Pitzer, J. Chem. Phys. 81 (1984) 356.

[35] 35 M. Peric, M. Petkovic, S. Jerosimic, Chem. Phys. 343 (2008) 141.

[36] L. Sari, J.M. Gonzales, Y. Yamaguchi and H.F. Schaeffer III, J. Chem. Phys. 114 (2001) 4472.

Tables

Table 1 - Vibrational frequencies (cm^{-1}) and relative intensities of the IR absorption bands observed for various isotopic species of $Cu(CO)_2$ isolated in solid argon (*italics for solid neon values*).

Assignment[a]	$Cu(^{12}CO)_2$	$Cu(^{12}CO)(^{13}CO)$	$Cu(^{13}CO)_2$	$Cu(^{12}C^{18}O)_2$
$2\nu_1$		4021.8		
$\nu_1 + \nu_3$	3914.9[b] *3939.3* (50)[c]	3872.1	3824.0	3830.8
$\nu_1 + \nu_4$	2542.5 *2562.0* (2.5)	2520.0	2491.1	2488.3
$\nu_2 + \nu_3$	2297 *2309.8* (0.8)	2262.8	2237.8	2232.8
ν_1	-	2031.0	-	-
ν_3	1890.9 *1904.5* (4880)	1865.9	1847.2	1850.1
?	888.4 (0.5)	-	878.7	886.3
$2\nu_{cis}$ bend	609.8 *610.6* (10)	600.8	592.0	603.3
ν_4	493 (1)	-	489.5	482.3
ν_{cis} bend	247.4 *247.8* (65)	243.5	240.2	245.2

a- Approximate description with Σ_g –modes: ν_1 CO stretch. and ν_2 Cu-CO stretch, Σ_u–modes: ν_3 CO stretch. and ν_4 Cu-CO stretch, Π_g –modes: ν_5 Cu-CO symmetrical bend, Π_u –modes: ν_6, ν_7 Cu-CO, C-Cu-C asymmetrical bend.

b- Argon value for the main trapping site, in italics for solid neon.

c- Relative intensities with respect to the 493 cm^{-1} weakest fundamental band.

Table 2 - Vibrational frequencies (cm^{-1}) and relative intensities of the IR absorptions of $Cu(CO)_3$ isolated in solid argon.

Assignment[a]	$Cu(CO)_3$	$Cu(CO)_2(^{13}CO)$	$Cu(CO)(^{13}CO)_2$	$Cu(^{13}CO)_3$	$Cu(C^{18}O)_3$
$\nu_1 + \nu_4$	4061.4 (w)[b]			4022.7	3971.5
$2\ \nu_4$	3943.0 (vw)			3853.8	-
$\nu_1 + \nu_5$	2545.6 (vw)			2489.1	
$\nu_1 + \nu_8$	2479.0 (vw)			2368.5	
$\nu_1 + \nu_6$	2420.5 (vw)	2408.6		2432	
$\nu_4 + \nu_8$	2354 (vw)			2297	
ν_4	1975.5 (s)	1956.5	1942.5	1930.7	1930.8
$2\nu_6$	630.9 (w)			611.8	
ν_5	443.5 (w)	≈440		437.6	
ν_8	378.5 (s)	≈374	≈370	368	374.5
ν_6	321.4(s)	≈322	≈318	312.1	319.4

a- Tentative assignment. A'_1 modes: CO, Cu-CO stretching modes (ν_1,ν_2), A'_2 modes: Cu-C=O in-plane deformation (ν_3), A''_2 modes: Cu-C=O, C-Cu-C out-of-plane deformations ($\nu_{8,}$ ν_9), IR-active, E' modes: C=O, Cu-CO stretch., Cu-C=O, C-Cu-Cu deformations (ν_4, ν_5, $\nu_{6,}$,ν_7) IR-active, E" modes: Cu-C=O out-of-plane deformations (ν_{10}).

b- S=strong, m=medium, w=weak, vw=very weak.

Table 3 - Comparison of experimental and calculated[a] harmonic frequencies for various isotopic species of $Cu(CO)_2$.

	$^{63}Cu(CO)_2$		$^{65}Cu(CO)_2$		$^{63}Cu(^{13}CO)_2$		$^{63}Cu(C^{18}O_2)$		$Cu(CO)\ ^{13}(CO)$	
	exp	calc	exp	calc	exp	calc	exp	calc	exp	calc
$\nu_1(\Sigma_g)$	2049.0[c]	2052.1	-	2052.1	2001.8[c]	2003.2	2005.7[c]	2007.2	2031.0	2031.0
$\nu_3(\Sigma_u)$	1890.9	1891.1	-	1891.1	1847.2	1846.5	1850.1	1849.4	1865.9	1865.4
$\nu_4(\Sigma_u)$	493.5	494.2	-	490.6	489.5	490.3	482.3	484.4	489	492.3
$\nu_2(\Sigma_g)$	406.6[c]	407.0	-	407.0	395.1[c]	400.6	382.2[c]	392.3	393.7[c]	403.7
$\nu_5(\Pi_g)$[b]	-	338.0	-	338.0	-	327.6	-	333.7	-	333.0
$\nu_6(\Pi_u)$	247.4	247.5	-	247.2	240.0	240.2	245.2	245.5	243.5	243.5
$\nu_7(\Pi_u)$[b]	-	70.2	-	69.8	-	69.4	-	68.7	-	69.8

a - F_{CO} = 15.22, F_{CuC} = 2.52, $F_{CO,CO}$ = 1.18, $F_{CuC,CuC}$ = 0.32, $F_{CuC,CO}$ = 0.3 mdyne $Å^{-1}$; F_{CuCO} = 0.235, F_{CCuC} = 0.1, $F_{CuCO,CuCO}$ = -0.092, $F_{CuCO,CCuC}$ = 0.0 mdyne Å rad^2 ; R_{CuC} = 1.73 Å, R_{CO} = 1.15 Å, Θ_{CCuC} = Θ_{CuCO} = 180°.

b - Set to the QC value, the same as predicted in this work.

c - Deduced from combination band and semi-empirical calculation.

Table 4. Some energetic, geometrical and electronic parameters at CCSD(T) structure. ρ and $\nabla^2\rho$ are given in e/Å^3 and e/ Å^5. Distances are in Å, angle in degree, binding energy (D_e at equilibrium structure and D_0 corrected for the vibrational frequencies) is in kJ/mol. Q^{net} = net charge, BCP = bond critical point.

Species	QTAIM topological analysis			Geometrical parameters	Binding energy
	Q^{net}(Cu)	BCP(CuC)	BCP(CO)		
CO			ρ = 0.489 $\nabla^2\rho$ = 0.337	R_{CO}= 1.135	
Cu-CO	+0.017	ρ = 0.092 $\nabla^2\rho$ = 0.309	ρ = 0.484 $\nabla^2\rho$ = 0.338	R_{CO}= 1.139 R_{CuC}= 1.976 Θ_{CuCO}= 150.3	D_e = -12.6 D_0 = -10.6
$Cu(CO)_2$	+0.416	ρ = 0.128 $\nabla^2\rho$ = 0.487	ρ = 0.470 $\nabla^2\rho$ = 0.273	R_{CO} = 1.150 R_{CuC} = 1.831 Θ_{CuCO} = 180	D_e = -77.5 D_0 = -66.9

Table 5. Harmonic vibrational frequencies (in cm^{-1}) and some force constants (in *mdyne/Å*) obtained at CCSD(T)/6-311+G(2d) level, compared to experimental frequencies in neon . For $Cu(CO)_2$, harmonic vibrational frequencies and intensities (*Km/mole*) calculated at B3LYP/6-311+G(2d) are also reported in parentheses.

	Calculated vibrational frequencies	Experimental
CO	ν_{CO} =2146 (2211) F_{CO}=36.5(38.7)	2143.2 (gas) , 2142.2 (Ne)
CuCO	ν_1(CO stretching) = 2072 , F_{CO} =17.0	2034.5 (Ne)
	ν_2 (CuC str./ OCCu bend)= 262	294.9 (Ne)
	ν_3 (CuC str./ OCCu bend) = 159, F_{CuC} = 0.65	176.7 (Ne)
$Cu(CO)_2$	$\nu_1(\Sigma g)$ = 2072 (2111, *0*)	2059.5[a]
	$\nu_3(\Sigma_u)$=2007 (1996, *4880*)	1904.5
	$\nu_4(\Sigma_u)$ = 489 (485, *1*)	502.5[a]
	$\nu_2(\Sigma_g)$ = 406 (388, *0*)	405.3[a]
	F_{CO} = 15.8 (15.65), F_{CuC} = 3.2(3.1)	610.6
	$\nu_{cis\text{-}XZ}$ = 380 (379,*1*), $\nu_{trans\text{-}XZ}$ =309 (303, *0*), $\nu_{c\text{-}Cu\text{-}C\text{-}XZ}$ = 67 (66, *1*)	
	$\nu_{cis\text{-}YZ}$ = 246 (243, *23*) $\nu_{trans\text{-}YZ}$ =374 (354,*0*), $\nu_{c\text{-}Cu\text{-}C\text{-}YZ}$ = 70 (72,*3*)	247.8

a- estimated from combination band

Figure Captions

Figure 1. Comparison of vibrational spectra for CuCO isolated in sold argon (top) and neon (bottom).

Figure 2. Comparison of vibrational spectra in the 2600-2440 cm^{-1} $\nu_1 + \nu_4$ combination region of $Cu(CO)_2$ for various isotopic precursor in solid argon.

Figure 3. Comparison of vibrational spectra in the 4400-3800 cm^{-1} $\nu_1 + \nu_3$ combination region of $Cu(CO)_2$ and for various isotopic precursor in solid argon. The asterisk designates the V=0-2 transition of $^{13}C^{18}O$ isotopic impurity.

Figure 4. Comparison of vibrational spectra in the 2100-1800 cm^{-1} region of CuCO, $Cu(CO)_2$, $Cu(CO)_3$ for various isotopic precursor in solid argon. The asterisk designates absorptions due to the $^{13}C^{18}O$ isotopic impurity.

Figure 5. Comparison of vibrational spectra in the 700-100 cm^{-1} region of CuCO, $Cu(CO)_2$, $Cu(CO)_3$ for various concentrations in solid argon. Cu/CO/Ar = 0.25/0.5/100 (a), 0.25/1/100 (b), 0.4/4/100 (c).

Figure 6. Comparison of vibrational spectra in the 280-220 cm^{-1} region of $Cu(CO)_2$ for various isotopic precursor in solid argon.

Figure 7. Comparison of vibrational spectra in the 670-470 cm^{-1} region of $Cu(CO)_2$ for various isotopic precursor in solid argon. The asterisks designates a CuO_2 impurity band.

Figure 8. Natural bonding orbitals evolving in the donation (from the occupied σ(C) to the unoccupied σ*(Cu) orbital) and back-donation (from the occupied σ(Cu) to the unoccupied π*(CO) and σ *(CO) orbitals) bonding modes in the bent Cu-CO molecule.

Figure 9. Natural bonding orbitals evolving in the formation of two σ(Cu-C) covalent bonds and in the back-donation (from the occupied π(Cu) to the unoccupied π*(CO) orbital) bonding modes in the linear $Cu(CO)_2$ molecule.

Figure 10. Schematic representation of the Renner-Teller potential energy surface for $Cu(CO)_2$ with $^2\Pi_u$ ground state.

Figure 1

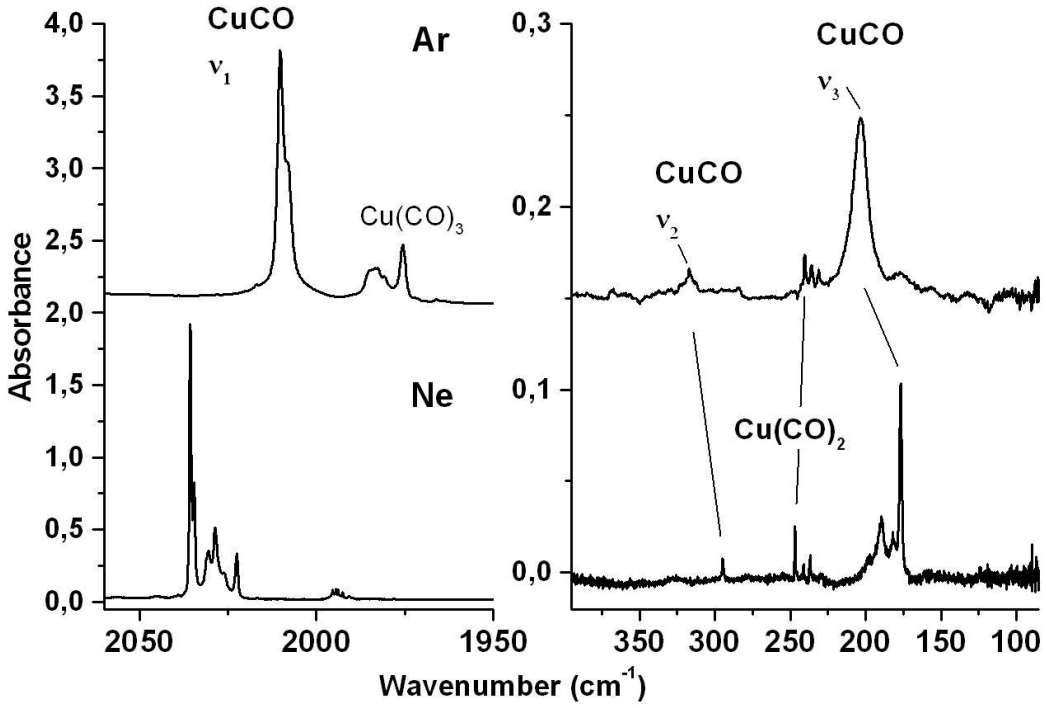

Figure 2

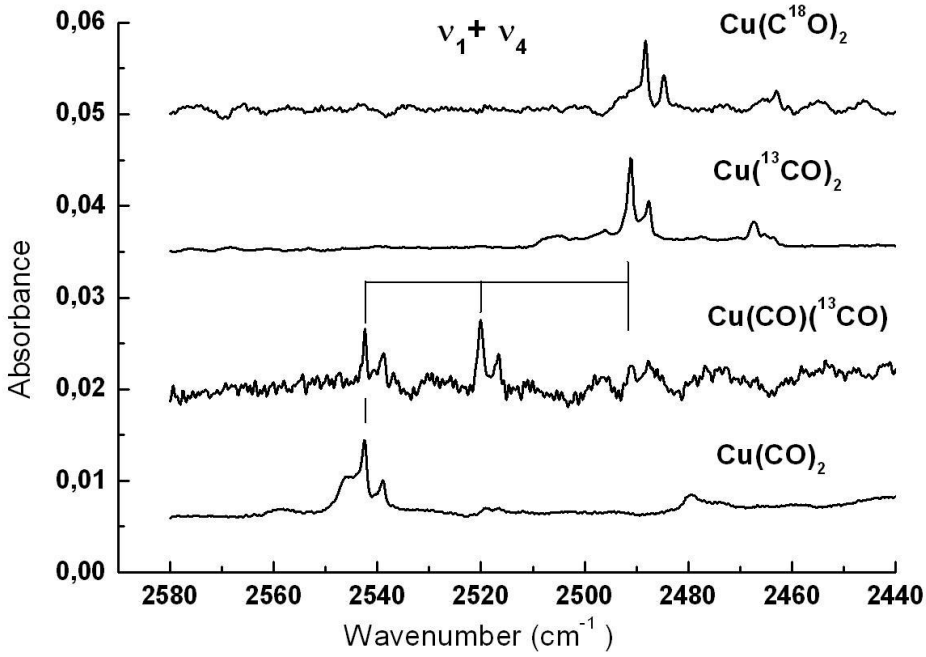

Figure 3

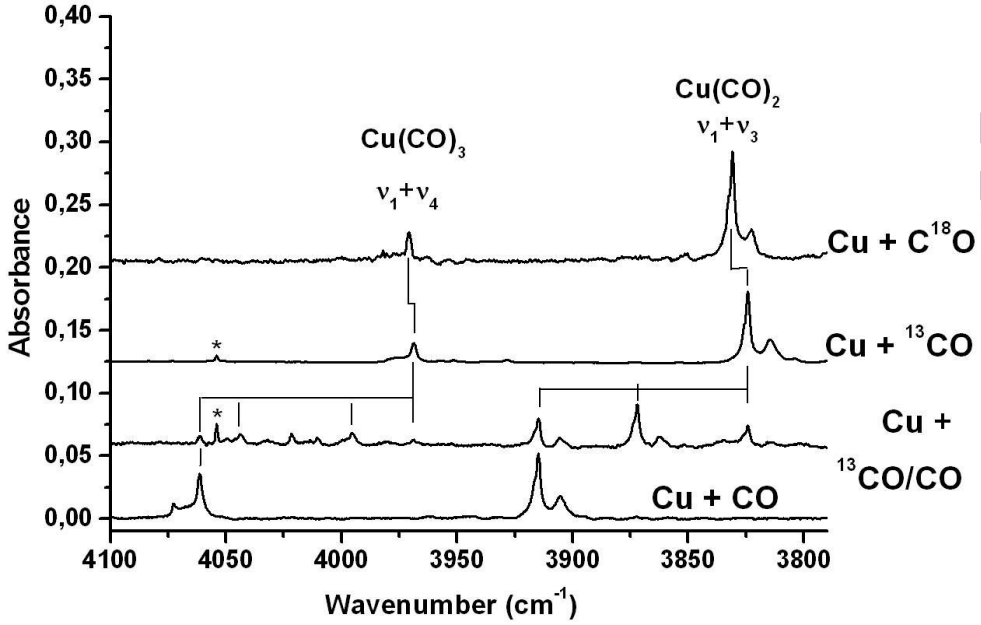

Figure 4

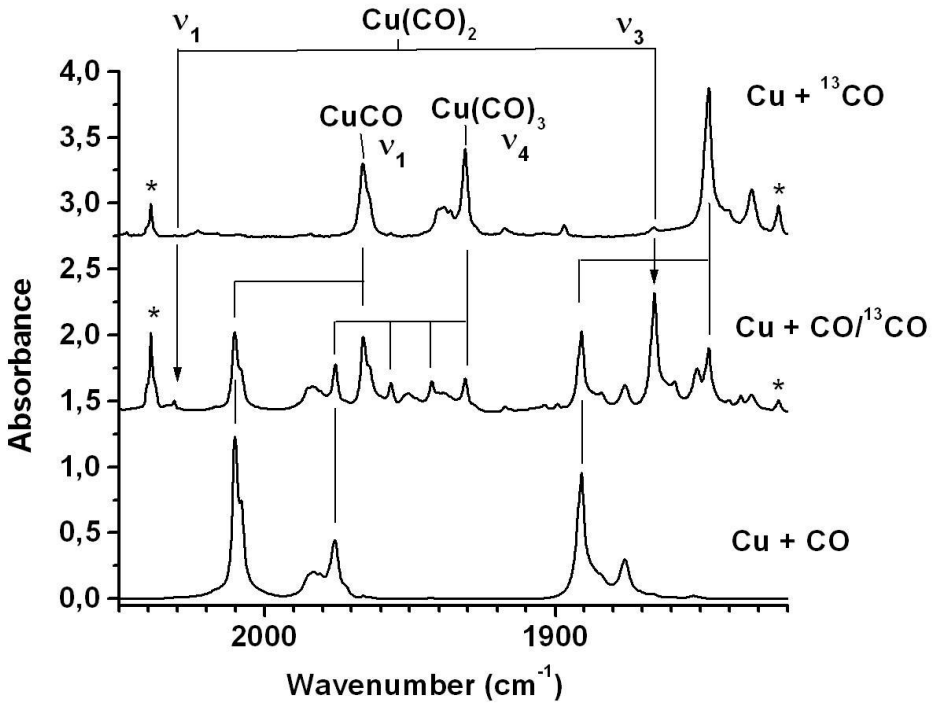

Figure 5

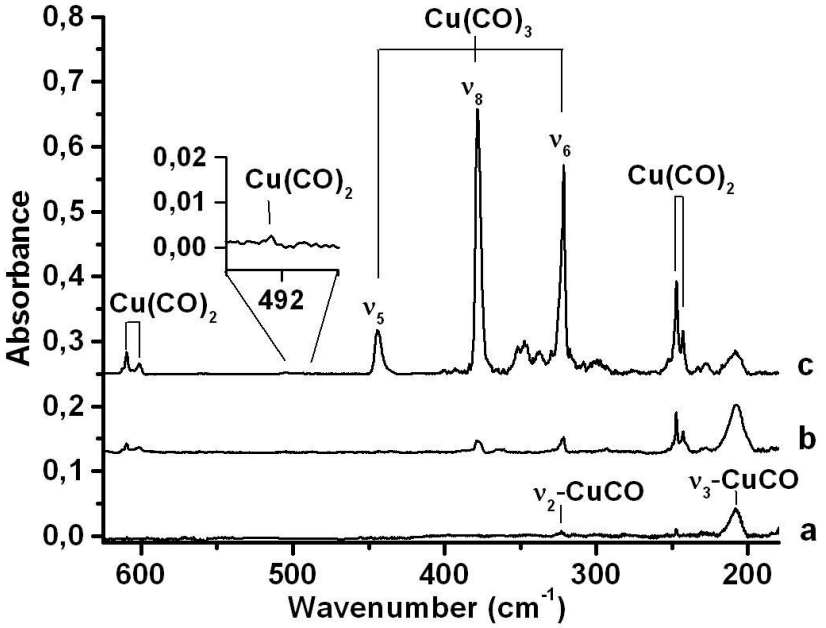

Figure 6

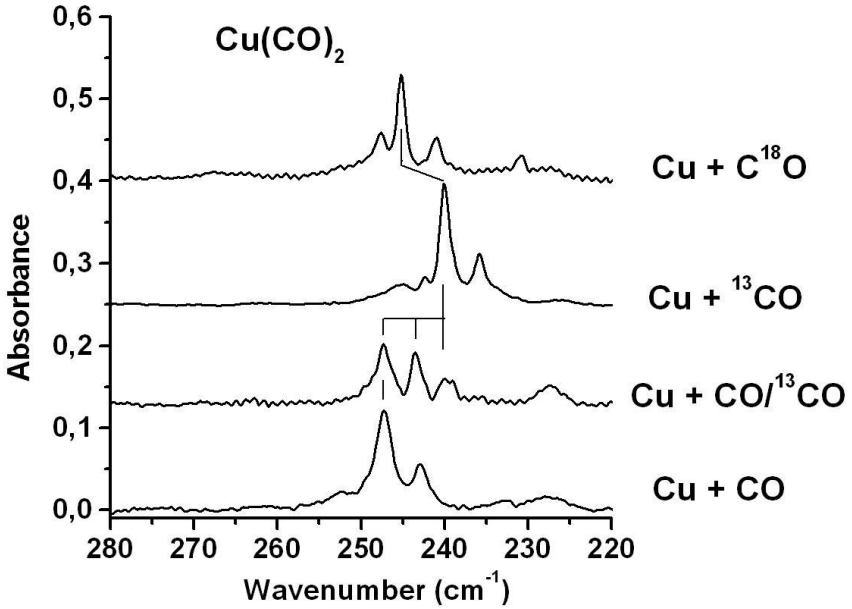

Figure 7

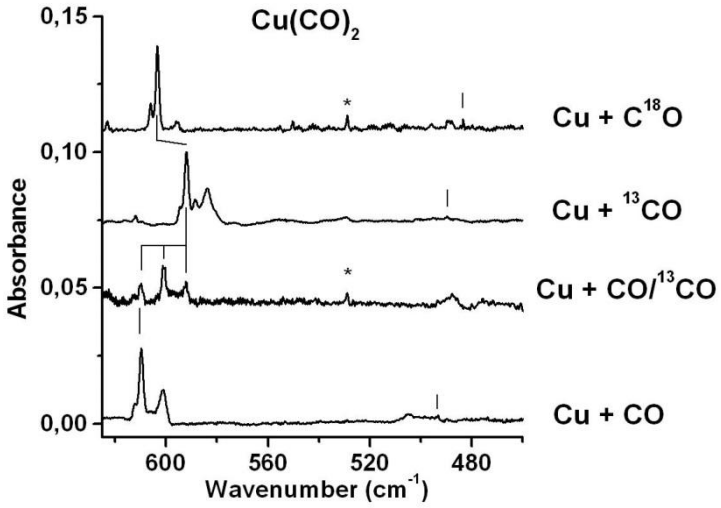

Figure 8

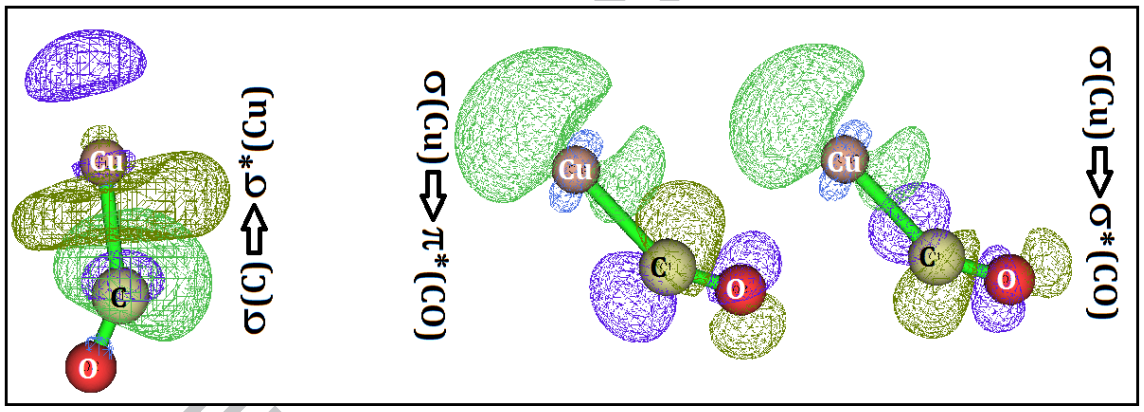

Figure 9

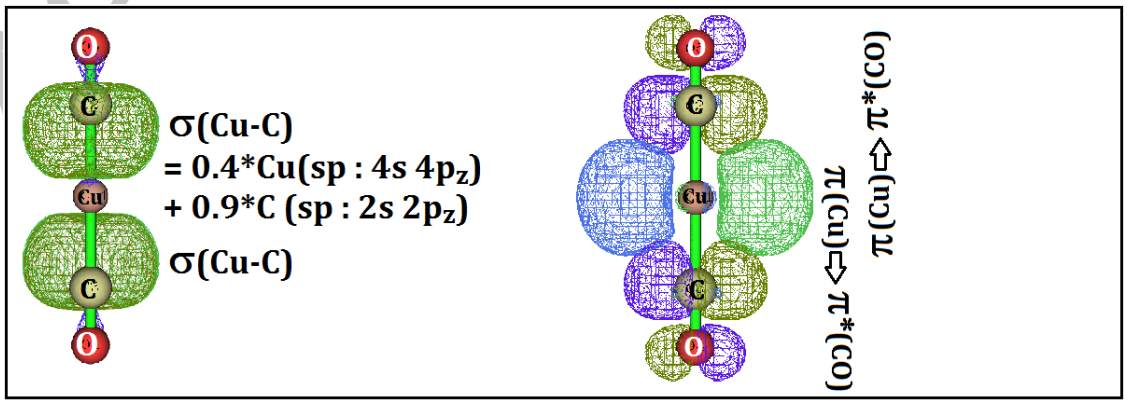

Figure 10

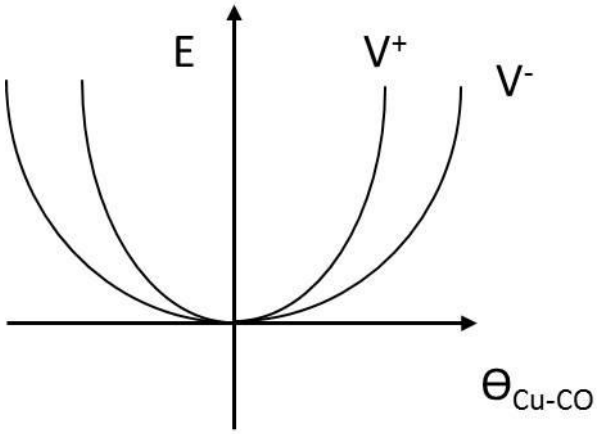

Highlights

- CuCO, $Cu(CO)_2$ isolated in solid argon and neon.

-$Cu(CO)_2$ a strongly bound and non-polar species.

-Vibrational data for all stretching modes of $Cu(CO)_2$

-Vibronic effects for bending modes due to Renner effect.

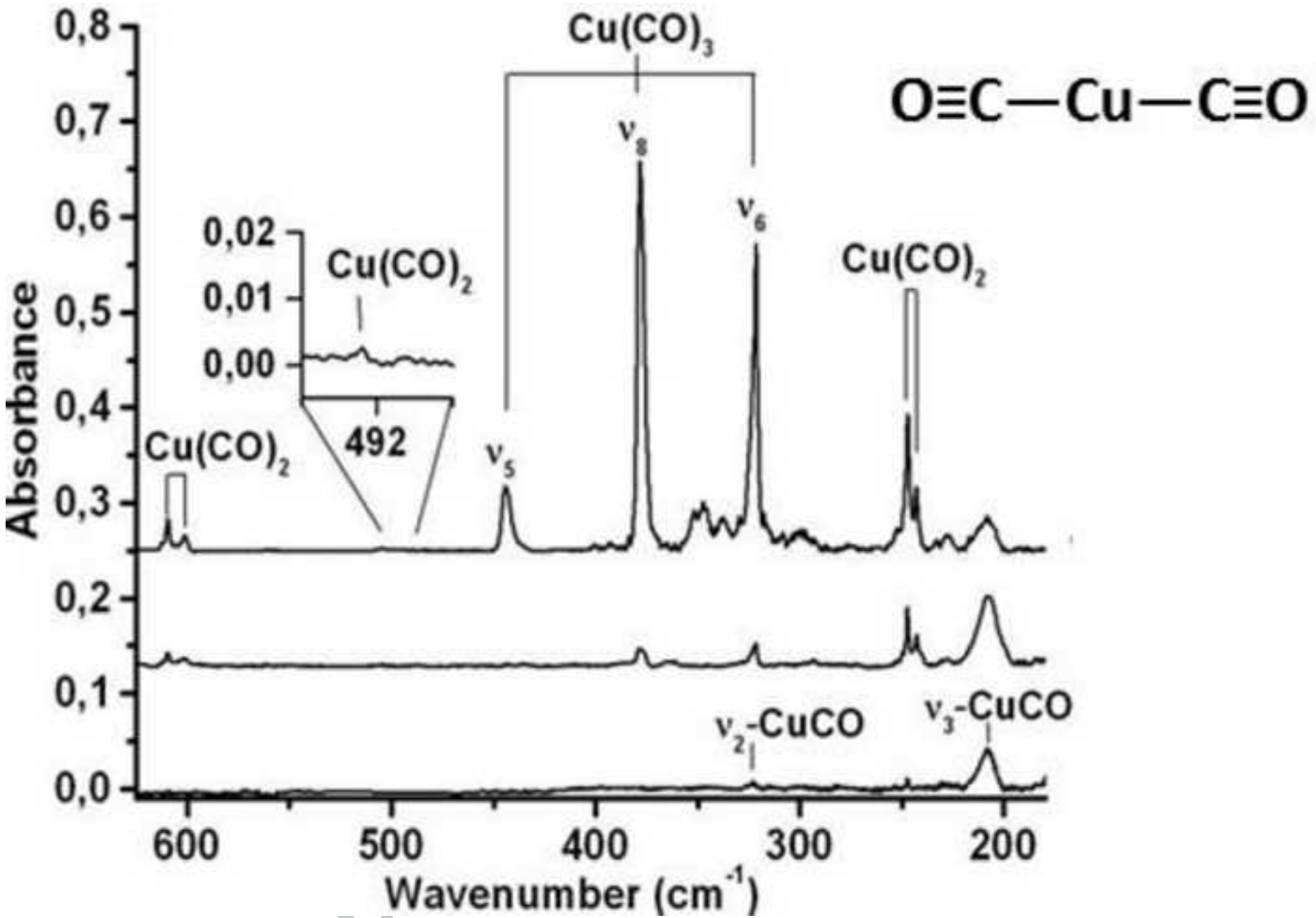
Cu(CO)3
O≡C—Cu—C≡O
ν8
ν6
Cu(CO)2
0,02
0,01
0,00
Cu(CO)2
492
Cu(CO)2
ν5
Absorbance
0,8
0,7
0,6
0,5
0,4
0,3
0,2
0,1
0,0
ν2-CuCO
ν3-CuCO
600
500
400
300
200
Wavenumber (cm-1)